ALMA MATER STUDIORUM
UNIVERSITÀ DI BOLOGNA

ARCHIVIO ISTITUZIONALE
DELLA RICERCA

Alma Mater Studiorum Università di Bologna
Archivio istituzionale della ricerca

The effect of organic and inorganic fibres on the mechanical and thermal properties of aluminate activated geopolymers

This is the final peer-reviewed author's accepted manuscript (postprint) of the following publication:

Published Version:
Giulia Masi, William D.A. Rickard, Maria Chiara Bignozzi, Arie van Riessen (2015). The effect of organic and inorganic fibres on the mechanical and thermal properties of aluminate activated geopolymers. COMPOSITES. PART B, ENGINEERING, 76, 218-228 [10.1016/j.compositesb.2015.02.023].

Availability:
This version is available at: https://hdl.handle.net/11585/474768 since: 2015-12-08

Published:
DOI: http://doi.org/10.1016/j.compositesb.2015.02.023

Terms of use:

Some rights reserved. The terms and conditions for the reuse of this version of the manuscript are specified in the publishing policy. For all terms of use and more information see the publisher's website.

This item was downloaded from IRIS Università di Bologna (https://cris.unibo.it/).
When citing, please refer to the published version.

(Article begins on next page)

12 October 2024

This is the final peer-reviewed accepted manuscript of:

Giulia Masi, William D.A. Rickard, Maria Chiara Bignozzi, Arie van Riessen, ***The effect of organic and inorganic fibres on the mechanical and thermal properties of aluminate activated geopolymers****, Composites Part B: Engineering, Volume 76, 2015, Pages 218-228, ISSN 1359-8368*

The final published version is available online at:
https://doi.org/10.1016/j.compositesb.2015.02.023

Rights / License:

The terms and conditions for the reuse of this version of the manuscript are specified in the publishing policy. For all terms of use and more information see the publisher's website.

This item was downloaded from IRIS Università di Bologna (https://cris.unibo.it/)

When citing, please refer to the published version.

G. Masi, W.D.A. Rickard, M.C. Bignozzi, A. van Riessen, The effect of organic and inorganic fibres on the mechanical and thermal properties of aluminate activated geopolymers. Composites Part B: Engineering 76 (2015) 218 – 228
doi:10.1016/j.compositesb.2015.02.023

The effect of organic and inorganic fibres on the mechanical and thermal properties of aluminate activated geopolymers

Giulia Masi [a,b*], William D.A. Rickard [b], Maria Chiara Bignozzi [a], Arie van Riessen [b]

[a] *Department of Civil, Chemical, Environmental and Materials Engineering, University of Bologna, via Terracini 28, 40131 Bologna, Italy*

[b] *Geopolymer Research Group, Curtin University, PO Box U1987, Perth, WA 6845, Australia*

Abstract

The addition of fibres to a brittle matrix is a well-known method to improve the flexural strength. However, the success of the reinforcements is dependent on the interaction between the fibre and the matrix. This paper presents the mechanical and microstructural properties of PVA and basalt fibre reinforced geopolymers. Moreover low density and thermal resistant materials used as insulating panels are known be susceptible to damage due to their poor flexural strength. As such the thermal and fire resistance properties of foamed geopolymers containing fibre reinforcement were also investigated.

The results highlight that the presence of PVA fibres greatly increased the flexural strength and the toughness of the geopolymer composite, while the presence of basalt

* Corresponding author. Tel.: +39 348 4017308; Fax: +39 051 2090361
e-mail address: giulia.masi5@unibo.it (Giulia Masi)

fibres improved the flexural behaviour of the composite after high temperature exposure.

Keywords

A. Fibres; E. Casting; D. Mechanical testing; B. Thermal properties.

1. Introduction

Geopolymer is a class of three-dimensional alumino-silicate material based on units such as sialate $[-\mathrm{Si}-\mathrm{O}-\mathrm{Al}-\mathrm{O}]$, sialate siloxo $[-\mathrm{Si}-\mathrm{O}-\mathrm{Al}-\mathrm{O}-\mathrm{Si}-\mathrm{O}]$ or sialate disiloxo $[-\mathrm{Si}-\mathrm{O}-\mathrm{Al}-\mathrm{O}-\mathrm{Si}-\mathrm{O}-\mathrm{Si}-\mathrm{O}]$ [1]. The polymerised materials contain tetrahedrally coordinated Al and Si, with charge balance of the Al tetrahedra being achieved by the presence of Na^+ or K^+ ions [2]. Geopolymers and alkali activated materials (AAM's) generally have attracted a lot of attention [3-5] as suitable alternative materials for constructions, due to their significantly lower CO_2 emissions during production [6]. A benefit of the use of geopolymer compared with ordinary Portland cement (OPC), the most commonly used building material, is the possibility of using high-volume industrial waste to manufacture geopolymer concretes, with a concomitant reduction in CO_2 emissions [7].

Fibre reinforcement has been used in various hardened binders to improve mechanical properties [8, 9]. Short fibres are one of the most commonly used reinforcement and are effective in improving flexural strength, toughness and in converting failure mode from brittle to ductile. Compared to continuous fibres, short fibres permit easier handling and manufacturing processes. Fibre aspect ratio and fibre

dispersion are the critical factors to consider when optimizing any improvement in strength.

Several studies assessing the mechanical performance of alkali-activated composites reinforced with different fibres have been reported in the literature [10 - 15] and some studies also investigated the thermal behaviour after high temperature exposure [4, 16 - 18]. Due to their durability, PVA fibres are one of the most commonly used reinforcement materials in ceramic composites for structural applications [19]. However, the exposure to high temperatures degrades PVA fibres, due to their organic composition. In the temperature range between 30°C and 1000°C, PVA samples exhibit three different weight loss stages that correspond to different phase changes: between 30°C and 210°C the loss of physisorbed water, between 210°C and 400°C the decomposition of the polymeric side chains and between 400°C and 540°C the decomposition of the main polymeric chain [20]. Basalt fibres are inorganic and as such have a much higher melting point (~1000 ^{o}C) than organic fibres making them a suitable candidate for high temperature resistant geopolymer composites.

Light-weight materials are often required for materials used in building applications, particularly in high rise construction. The use of geopolymers of lower density is beneficial in terms of reduced structural load-bearing with further benefits of improved acoustic and thermal insulation [21, 22]. However, the trade-off is that low density geopolymers generally exhibit low strength [1].

Different foaming agents can be used to synthesise low density geopolymers. For instance, chemical products which react with the alkali to generate gas [23], metals, such as zinc or aluminium, which generate hydrogen gas [23, 24] and metallic silicon

present as an impurity in silicon carbides or silica fume also generates hydrogen gas when exposed to alkali [25, 26]. Another class of chemical foaming agents is peroxides such as hydrogen peroxide and organic peroxides which react to evolve oxygen gas [24]. Bubbles of O_2 are trapped within the paste, resulting in lower density.

It is known that low density materials have low thermal conductivity and are more suitable for thermal insulation exposure [4]. Materials designed for refractory and fire resistance applications must be able to be exposed to high temperature for extended periods while retaining physical properties such as strength.

This paper presents a study where foamed geopolymers have been reinforced with two different types of fibres: organic (PVA) and inorganic (basalt) short fibres. Fibres have been introduced with the aim of modifying the brittle fracture behaviour of geopolymers. Low density formulations were synthesised using hydrogen peroxide and a chemical surfactant, exploiting the best results of a previous study [27].

First, mechanical, physical and microstructural properties are reported as well as the thermal behaviour of fibre reinforced geopolymers (FRGP) in order to assess the suitability of the different fibres in geopolymer composites. Then, thermal conductivity measurements and fire testing was performed on foamed and fibre reinforced geopolymers (FFRGP) in order to understand the behaviour of the different fibres in composites with low density matrices for possible thermal insulation applications.

Composite materials based on geopolymer matrices can be produced for various applications requiring good performances at elevated temperatures [16, 17, 28, 29], but also for applications where thermal insulation [30] at room temperature is necessary

(e.g. blocks and plaster for the building sector). The addition of short fibres in low density geopolymers also stabilizes the foam during synthesis by increasing the viscosity of the paste and consequently reducing pore collapse [4].

2. Experimental

2.1 Materials

Fly ash was sourced from Eraring power station in New South Wales, Australia. Sodium aluminate solution was used as the alkali activator. Solutions were prepared by dissolving sodium hydroxide pellets from Univar Pty Ltd and sodium aluminate powder supplied by Sigma-Aldrich in deionised water. The chemical composition of sodium aluminate used in this study was Al_2O_3 50 wt%, Na_2O 50 wt% and some impurities of Fe_2O_3 (<0.05 wt%). The pellets and powder were allowed to dissolve overnight at 70°C and used for synthesising geopolymers after 24 h. Activator solutions were characterised by Na_2O:Al_2O_3 = 0.5 and H_2O:Na_2O = 2,1. PVA short fibres (Nycon-PVA RECS 15, Australia) 8 mm long and 38 μm in diameter and basalt chopped fibres (Technobasalt, Ukraine) 5 mm long and 16 μm in diameter were used as the fibre reinforcement. Hydrogen peroxide solution with 30 wt% supplied by Rowe Scientific was used as the chemical foaming agent. Sika® LIghtcrete 02 was used as the surfactant for foam stabilization.

2.2 Geopolymer synthesis

Geopolymers were synthesised with targeted compositional ratios of Si:Al=2.0, Na:Al=1.1 and a water content of 21 wt%. Samples were made by mixing the fly ash with the activating solution for 10 min. Fibre reinforced geopolymer (FRGP) were

synthesised by adding different concentrations of fibres (0.5 vol% and 1.0 vol%) after 5 min of the initial mixing time and mixed for another 5 min. Foamed and fibre reinforced geopolymer (FFRGP) samples were produced by foaming the pastes with surfactant and hydrogen peroxide (1 wt% of surfactant added at 5 mins together with the fibres, and 0.1 wt% of hydrogen peroxide added after 10 mins and mixed for a further 20 s). Immediately after mixing samples were poured into moulds, sealed and cured at 70°C for 24 h.

2.3 Physical testing and microstructure

Workability was measured using a mini-cone slump tester (57 mm high, with 19 mm and 38 mm top and bottom diameters, respectively). Geopolymer slurry was poured to fill the cone and after lifting the cone up, the slurry was allowed to flow for 1 min prior to measuring the diameter.

The density of the samples was measured by dividing the dry mass by the volume. Cylindrical samples (50 mm diameter, 100 mm high) were used for density measurements. All reported results are an average of measurements from 4 samples.

Pore size distribution measurements were carried out on all specimens by a mercury intrusion porosimeter (MIP, Carlo Erba 2000) equipped with a macropore unit (Model 120, Fison Instruments). Samples for porosimetry were cut by diamond saw to approximately 1 cm^3, dried under vacuum and kept under a P_2O_5 atmosphere in a vacuum dry box until testing. The MIP measurements were carried out using a contact angle of 141.3° and Hg surface tension of 480 dyne/cm. The suitability of MIP for pore size and pore size distributions is frequently debated [31 - 33], however its use in

cement based materials is accepted [34-36] and it is also becoming common in the field of inorganic polymers [37 - 39].

Scanning electron microscopy (SEM) was conducted on a NEON 40EsB (Zeiss, Germany) field emission SEM. Sample fragments of FRGP were mounted onto aluminium stubs and out-gassed in a desiccator over a 24 h period. The samples were then coated with a 5 nm layer of platinum prior to imaging.

2.4 Mechanical testing

All the mechanical tests were conducted by means of a Lloyd universal tester EZ50 on FRGP after 7 days of storage at room temperature in plastic bags (i.e. 100% rH). This time was selected as it is the time after which most of the mechanical properties have been developed in geopolymers cured at elevated temperatures [18, 40]. Cylinders of 25 mm diameter and 50 mm height were prepared for compressive strength testing. A load rate of 0.25 MPa/s was used to comply with ASTM C39 [41]. Flexural strength and fracture toughness tests were performed on 20x20x90 mm cuboids. Flexural strength testing was conducted in ~~close~~ accordance with ASTM C78 [42] and fracture toughness was conducted in ~~close~~ accordance with ASTM C1421-10 [33]. A span of 40 mm was set up for the three points bending tests and a preload force of 50 N was used to ensure no movement during the specimen testing and a load rate of 1 mm/min was used. Before the fracture toughness testing, samples were prepared by creating an initial crack with a depth of 4 mm and a thickness of 0.1 mm width. The values for fracture toughness of each samples was calculate using Eq. (1) [43]:

$$K_{Ipb} = g\left(\frac{P_{max}S_0 10^{-6}}{BW^{3/2}}\right)\left[\frac{3(a/W)^{1/2}}{2(1-a/W)^{3/2}}\right] \quad (1)$$

where K_{Ipb}= fracture toughness for each specimen (MPa$\sqrt{m}$); P_{max} =maximum force (N); S_0 = span (m); B = width of the test specimen; W = thickness of the test specimen; a = crack length (m); g = g (a/W) = experimental function of ratio between crack length and thickness of the specimen.

The stated strength and fracture toughness values for all the mechanical tests are the average of results of measurements from 4 samples.

2.5 Thermal characterization

Thermal conductivity was measured on FFRGP using the transient hot wire method [4]. The tests were conducted by placing a 0.32 mm thick nickel-chromium heating wire moulded between two halves of one of the cylindrical samples (50 mm diameter, 100 mm height). A potential difference of 2.0 V and current of 1.0 A was used to heat the strip and temperature increase was measured using an embedded K-type thermocouple. The temperature was logged for 15 min and the thermal conductivity (k) was calculated using Eq. (2) [44]

$$k = \frac{VI}{4\pi La} \quad (2)$$

where k= thermal conductivity (W/mK), V= voltage (V), I = current (A), L = length (m) and a = gradient of temperature rise versus the natural log of the time in seconds.

A custom designed electric furnace was used for the fire testing on FFRGP (further details are available in Rickard et al. [4]). The sample exposure region was 200x200

mm. The heating regime followed a fire curve in accordance with ISO 834 [45]. The temperature was controlled using a multi stage controller (model PAK-700, Furnace technologies Pty Ltd) programmed to follow the time-temperature relationship described Eq. (3)

$$T = 345\log_{10}(8t - 1) + 20 \qquad (3)$$

where T = temperature (°C), t = time (min).

Three K-type thermocouples were placed onto the cold side of the sample. Cold side temperatures were recorded individually and as the average of the three thermocouples. The data for the thermocouples was logged every 5 s using a Vernier LabQuest (U.S.A.).

3. Results

3.1 Physical properties

Increasing the concentration of PVA fibres in the paste greatly increased the viscosity of the slurries. It was found that adding 1.0 vol% of PVA fibres resulted in a flowability loss of more than 40% (Table 1). This significant loss in flowability of the fresh slurry created difficulties in casting the samples and reduced the cured density by increasing the propensity for air entrainment (Table 1).

The workability was not significantly affected by adding 0.5 vol% of basalt fibres, whereas the presence of 1.0 vol% of basalt fibres reduced the slurry flowability by 26% (Table 1). This relatively small loss of slurry workability was likely due to the smaller

aspect ratio and the smoothness of the surface of the fibres (Fig. 3) and caused no significant change in density when increasing the content of basalt fibres indicating that air entrainment was minimal.

Fibre reinforced geopolymers were also foamed using a combination of surfactant and hydrogen peroxide. From previous investigations [27], the combination of surfactant and hydrogen peroxide was found to improve the properties of low density geopolymers, achieving the best control of density and porosity. Both the FFRGP samples exhibited, after curing, a density around 1.0 g/cm^3, as reported in table 2. Density values of both FFRGP panels are comparable and this made the combination of the foaming agents used suitable for achieving similar physical properties of foamed geopolymers reinforced with different short fibres. The presence of fibres resulted in a more viscous mix thus reducing the susceptibility for pore collapse and making the casting of the samples easier.

3.2 Mechanical properties

The presence of PVA or basalt fibres was not found to affect the compressive strength values of FRGP, which was measured to be approximately 20 MPa. FFRGP exhibited compressive strengths of 5 MPa and 4.5 MPa for samples reinforced with PVA and basalt fibres, respectively. Due to the ductile behaviour of PVA, the mode of failure during compressive strength testing of PVA fibre reinforced samples was different compared to that one shown by pure geopolymers and samples reinforced with basalt fibres. Instead of a sharp drop in the stress-extension graph at the point of maximum load, typical of the failure mode of the geopolymer matrix and basalt fibre reinforced samples, geopolymers reinforced with PVA fibres exhibited an extended

period of plastic deformation (Fig. 1). The PVA fibre reinforcement allowed the samples to support some load even after the initial failure created extensive cracking in the structure.

The addition of PVA fibres had a direct influence on improving the flexural strength of the matrix (Fig. 2-A). This was likely due to the high tensile flexural strength of the fibres and to their crack-bridging behaviour probably due to the adhesion to the geopolymer matrix. This was caused by the fibre debonding process that occurred along the fibre/matrix interface and allowed a more efficient load transfer mechanism. Moreover the reinforcement with PVA fibres clearly contributed to an increase in the area under the non-linear portion of load-deflection curve reflecting changing failure behaviour from a brittle mode to a ductile one (Fig. 1). All the samples exhibited a first breaking point in the range 600 - 800 N that corresponded to the brittle failure of the geopolymer matrix, however the presence of PVA fibres significantly increased the energy absorbed during the loading period. The energy absorbed by the 0.5 vol% PVA fibre reinforced geopolymers was 7 times greater than the geopolymer matrix alone and the concentration of 1.0 vol% of PVA fibres showed double the work values of the 0.5 vol% samples, as shown in Fig. 2-C. This was due to the ductile behaviour of PVA fibres and their higher flexural strength compared to the geopolymer matrix. The increased ductility of the samples reinforced with PVA fibres was likely to have resulted from fibre pullout, after fibres stretched, due to their high tensile strength.

The presence of chopped basalt fibres in the geopolymer matrix did not influence the flexural behaviour, as shown in Fig. 2-A. The basalt fibres used in this study had greater tensile and flexural strength than PVA though they suffer brittle failure mode and as

such did not improve the breaking behaviour of the composite. However, adding 1.0 vol% of basalt fibres to the geopolymer matrix resulted in a small increase of the energy absorbed during the three point bending test. The values of strain to failure to 1.5 mm sample extension of basalt FRGP (1.0 vol%) showed an improvement of 53% compared to the strain of failure to 1.5 mm extension of non-reinforced geopolymer matrix (Fig. 2-C).

The ductile behaviour of PVA fibres and the presence of basalt fibres imparted an improvement in fracture toughness values (Fig. 2-B). In particular, presence of basalt fibres in the geopolymer matrix increased the values of fracture toughness by 45% for 0.5 vol% of basalt fibres and 74% for the 1.0 vol%.

Similar fracture toughness values were reported in literature for metakaolin geopolymer concrete reinforced with basalt fibres: fracture toughness values of 0.046 $MPa \cdot m^{0.5}$ were observed for the geopolymer concrete. The presence of 0.5% of basalt fibres in the composite did not significantly improve the values of fracture toughness that were around 0.058 $MPa \cdot m^{0.5}$. Values around 0.091 $MPa \cdot m^{0.5}$ were observed for 1.0% of basalt fibres in geopolymer concrete [46].

3.3 Microstructural properties

SEM images of PVA fibre reinforced geopolymer showed good adhesion between the matrix and the fibres (Fig. 3-A). Longitudinal striations on the PVA fibre surfaces led to increased adhesion of the paste to the fibres. Most of the fibres were covered by the geopolymer gel and their surfaces showed more striations and some peeling when

compared with original surfaces (Fig. 3-B). This was likely due to chemical bonding that is the reaction of fibre surfaces with alkali present in the activator.

The ends of the fibres pulled out from the matrix were mostly covered by the matrix. This is an indication of fibre pull-out from the matrix and indicates strong adhesion between the geopolymer gel and the surface of the fibre. Other studies reported that the fibre failure mode or fibre pull out from the matrix is strongly influenced by the bond between fibres and matrix. Moreover it was noted that fibre pull out happens when the interfacial zone is poorly evident whereas a clear interfacial zone produces a fibre fracture mode of failure [47].

Fig. 4 shows basalt fibres in the geopolymer matrix. The original basalt fibres were observed to have smooth surfaces, which did not change after being incorporated into the geopolymer matrix. This indicates that the caustic in the activating solution did not significantly degrade the fibres. A purely physical bond likely occurred between basalt fibres and geopolymer matrix. The fibres did not appear to have reacted with the matrix and most of the fibres were only partially covered by the geopolymeric particles. The lack of geopolymer gel in the surface of pulled out fibres suggests the bonding with the matrix was weak. The ends of the fibres showed sharp cross-sections that are an evidence of brittle failure.

3.4 Thermal behaviour

Flexural strength values after high temperature exposure are reported in Fig. 5 for both the fibre reinforcements. Different ranges of temperatures were used in order to investigate where the fibres started to degrade. PVA fibre reinforced geopolymers

exhibited constant flexural strengths of 14 MPa until the samples were exposed to temperatures greater than 150°C. Temperatures of 200°C and 250°C caused a decrease in values of flexural strength of 35% and 70%, respectively. Moreover, raising firing temperature above 200°C resulted in a loss of ductile failure mode, that characterized PVA fibre reinforced geopolymers (Fig. 5-C and Fig. 5-D). This behaviour is due to the physical changes of PVA fibres during high temperature exposure.

As the melting point of basalt is 1000°C [48], a range of higher temperatures was used for sample exposure prior to the three points bending test. It was observed that flexural strength did not change significantly in the range of 600°C and 700°C from the samples tested as cured. However, beyond 700°C the flexural strength values nearly doubled. This improvement in flexural strength is likely caused by the sintering of the geopolymer paste leading to an improved fibre-matrix adhesion.

Fig. 6-A shows a PVA fibre in the geopolymer paste after exposing the samples to 250°C. The fibre exhibited an irregular shape with respect to the cylindrical morphology observed before firing. This indicates the PVA fibres started to become viscous and shrink at temperature~~s~~ higher than 200°C: detachment of fibres from the matrix will occur, as is clearly visible in Fig. 6-A, and thus the fibres no longer provide reinforcement to the composite.

The microstructure of basalt fibre reinforced geopolymers was investigated at each temperature to assess the effects of the fibres in the geopolymer paste (Fig. 6). When compared with the microstructure of unfired samples, which is characterised by geopolymer gel amongst unreacted fly ash particles, fired samples appeared more reacted and coarse pores were present throughout. High temperature exposure (up to

800°C) causes sintering within the geopolymer phase, which improved the bonding both within the geopolymer matrix and between the matrix and the basalt fibres. Other studies recorded similar behaviours for geopolymer-based paste exposed at high temperatures [18]. The fibres did not exhibit any observable degradation due to firing from 600°C to 1000°C.

Thermal conductivity of FFRGP is reported in table 3. The solid (not foamed) geopolymer paste exhibited a thermal conductivity value of 0.53 W/mK. It was observed that decreasing densities achieved lower thermal conductivity values due to the presence of more air voids, that have low thermal conductivity [49]. The values measured in this study were comparable with ones reported for foamed Eraring fly ash geopolymers where a density of 0.93 g/cm^3 produced a thermal conductivity of 0.25 W/mK [4]. Many of the reported thermal conductivities of geopolymer foams in the literature are lower than the ones measured in this study; this can be attributed to the lower densities of those samples compared to the ones produced in this research [16, 50].

Fire tests were conducted to assess the ability of the samples to insulate the heat from a simulated fire. Tests were conducted for 180 min as this was enough time to exceed the maximum temperature increase allowable by testing standard (ISO 834, AS 1530.4). The following conditions were used to determine the fire rating of the samples [51]: failure condition 1 - average temperature of the cold side of the sample exceeds 165°C; failure condition 2 – the temperature at any location of the cold side of the sample is greater than 205°C.

The two geopolymer samples exhibited similar trends in the cold side curves during the fire test (Fig. 7-A and Fig. 7-B): 10 min from the start of the test, the cold side temperature remained at ambient temperature and after that it began to increase. When the cold temperature approached 100 °C the temperature rise decreased to form a plateau. This was due to the passage of the boiling front through the top of the sample [4, 30]: as the sample was heated, the water contained inside the pores of the geopolymer, expanded and this generated pressure within the pore network, forcing the water to flow away from the top of the sample. The boiling point plateau is caused by the energy carried away by the evaporation of water as is reaches the top surface of the sample. This causes the measured temperature to remain constant until all the evaporable water is removed from the sample. The last stage shows an increase of the cold side temperature once all the water has evaporated from the sample.

Fig. 7-C compares the average cold side temperatures of FFRGP panels reinforced with PVA and basalt fibres. It was observed the two samples exhibited similar trends with the difference that the basalt fibre reinforced panel got to the boiling front plateau faster compared to the PVA fibre reinforced one. This is partly due to its higher thermal conductivity. In addition, when PVA fibres started to degrade there were channels left inside the panel; this facilitated moisture transfer and thus reduced the period for the boiling front to move through the sample.

Table 4 reports the times when the samples exceeded the failure conditions. The hot side of the samples was subjected to a maximum temperature of almost 1100°C during the 180 min fire test, whereas the cold side increased to approximately 240°C for both the panels. It was observed the panel reinforced with PVA fibres exhibited higher

resistance (in terms of time) for both the failure conditions compared to the sample reinforced with basalt fibres. The results achieved for these samples were better than ones presented in other studies on fly ash geopolymers [4, 30]. The mass loss of the two panels after fire exposure are reported in Table 4 and it was found that both samples had similar mass loss value. The foamed PVA fibre reinforced panel exhibited slightly higher mass loss, likely due to degradation of PVA fibres during the test; whereas basalt fibres can be still observed in the sample after fire exposure.

Fig. 8 reports pore size distributions of three different portions of the cross section of FFRGP panels after fire testing. In particular sample portions extracted near the hot side, near the cold side and in the middle of the panels were used for MIP measurements, in order to understand the changes in porosity in the cross section of the panels. For both samples, a decrease in volume of micropores was recorded for the portion near the hot side of the panels. This is caused by the coalescence of micropores due to the densification of the sintered matrix. In addition, the sample reinforced with PVA fibres exhibited an increase of macropores near the hot side. This is due to the presence of pore created after the degradation of PVA fibres during fire testing.

Fig. 9 shows the hot and cold side of the panels of FFRGP. Both the samples exhibited cracks on their “hot and cold” surfaces after the fire test. The cracks were not observed to form on the cold side of the samples until after the initial dehydratation period finished (about 60 min into the test). This suggests that the evaporation of the water did not cause extensive damage. It is likely that the major cause of cracking on the cold side of the sample was due to the differential shrinkage of the hot side with respect to the cold side as the parts of the sample that were hot enough to sinter would

have shrunk much more than the cooler regions, causing the cracking. Moreover, different crack patterns in the hot side of the two panels were observed: the sample with PVA fibres exhibited a denser distribtion of smaller cracks compared to the panel with basalt fibres. This was likely due to the decomposition of PVA fibres that could create dehydration pathways for water thus reducing cracking and spalling. The cracking on the hot side was found to be relatively shallow, in particular in the samples with the PVA fibres.

The cross-sections of the tested panels are shown in Fig. 10. A 10 mm yellow to orange layer can be distinguished in both the panels, where the iron oxides presented in the fly ash have been exposed to high temperature and consequently oxidised. After the fire test, both the panels were stable; indeed none of the cracks affected the whole thickness of the panels.

4. Discussion

Compressive strength of the geopolymer was not affected by the addition of either PVA or basalt fibres. PVA fibre reinforcement produced consistent improvement of flexural strength values as well as fracture toughness when the concentration of fibres was increased. The individual values for fracture toughness of 1.0 vol% PVA fibre reinforced geopolymers were very variable, probably due to uneven dispersion of the fibres and the challenge of maintaining random orientation of the fibres in very viscous mixes. This was shown in greater loss in flowability when the concentration of PVA fibres was increased. The mechanical improvements in the PVA reinforced geopolymer samples were believed to be caused by fibre pull out which allowed for ductile failure of the composite. The results suggest a more favourable interaction between PVA fibres

and the matrix than the basalt fibres, possibly due to a combination of physical and chemical bonding.

Geopolymer samples reinforced with basalt fibres exhibited no significant loss of workability when increasing the concentration of basalt fibres. This was likely due to low aspect ratio of the basalt fibres and also their smooth surfaces. No significant improvements in mechanical properties were measured in the composites, likely due to low bonding between the matrix and the fibres. All the samples exhibited a brittle failure mode during mechanical testing. The addition of organic (PVA) and inorganic (basalt) fibres produced geopolymer-based composites characterised by very different physical and mechanical performance, similar to what happen in cementitious materials. This is primarily due to a completely different interaction between the fibre and matrix. As PVA is hydrophilic, fibres exhibit high bond strength in cementitious binders [52, 53], due to hydroxyl groups that result in a strong hydrogen intermolecular bond; in other words there is a chemical bond between PVA fibres and the matrix [53]. Conversely, basalt fibres in an alkaline environment, as occurs in cement and geopolymer matrices, exhibit excellent corrosion resistance (i.e. have minimal chemical interaction with the matrix). In particular, the presence of Al_2O_3 and SiO_2 produced a film over the fibre surface that improves the alkaline resistance and leads to a physical bond with the cementitious matrix instead of a chemical fibre/matrix bond [54].

After exposing the fibre reinforced samples to high temperatures (from 100°C to 250°C for PVA FRGP and from 600°C to 1000°C for basalt FRGP), different mechanical behaviour was observed. The degradation of PVA fibres caused the loss of most of the flexural resistance and of the ductile failure mode. The basalt fibres did not

degrade until 1000°C and the composites increased in flexural strength due to the improved bonding with the matrix after sintering.

Thermal properties of fibre reinforced geopolymers that have been foamed with a combination of surfactant (1.0 wt%) and hydrogen peroxide (0.1 wt%) were investigated. The fire testing showed that the time taken for the samples to exceed the failure condition was dependant on density, as well as thermal conductivity values. As the foamed samples reinforced with PVA or basalt fibres exhibited comparable density values, it could be stated that the nature of the fibres added did not influence the performance of geopolymers under simulated fire conditions. Fire rating of the samples at 50 mm thickness was 80 - 100 min and the best performing sample was the foamed PVA fibre composite.

5. Conclusions

Physical and mechanical properties of fly ash-based geopolymers reinforced with PVA or basalt fibres have been presented. High temperature behaviour of FFRGP has also been described. Organic fibres (PVA) are a suitable reinforcement for room temperature applications achieving flexural resistance and avoiding total collapse of the sample during mechanical testings by virtue of the ductile failure mode of the PVA fibres. Inorganic fibres (basalt) did not significantly improve mechanical properties of the composite, due to the limited bonding with the matrix and the brittle failure of the fibre. However, basalt fibres are more suitable for thermal applications in a range of higher temperatures compared to PVA fibres that started to degrade above 150°C.

Foamed and fibre reinforced geopolymer composites have potential in applications such

as insulators or as light weight building materials. Foaming the samples improved their ability to insulate due to a sample density of 0.96 g/cm^3 and an associated 30% reduction in thermal conductivity. For the fire rating test, the best performance were observed for the foamed PVA fibres composite, thus indicating that PVA fibres degradation can be functional to reach good fire resistance products.

Acknowledgements

This study was supported by Curtin University and the R&D Centre for Valuable Recycling (Global-Top Environmental Technology Development Program) funded by the Ministry of Environment, South Korea (Project No. : GT-11-C-01-280-0). The authors acknowledge the use of equipment, scientific and technical assistance of the Curtin University Electron Microscope Facility, which is partially funded by the University, State and Commonwealth Governments. The authors would also like to thank Emily Xie for her assistance with the laboratory work. The author Giulia Masi would also like to thank the University of Bologna for the grant to support the study during her Master's thesis.

References

1. Davidovits J. Geopolymers. J. Therm. Anal. Calorim. 1991; 37 (8): 1633-1656.

2. Barbosa VF, MacKenzie KJ. Thermal behaviour of inorganic geopolymers and composites derived from sodium polysialate. Mater. Res. Bull. 2003; 38 (2): 319-331.

3. Natali Murri A, Rickard W, Bignozzi MC, van Riessen A. High temperature behaviour of ambient cured alkali-activated materials based on ladle slag. Cem. Concr. Res. 2013; 43: 51-61.

4. Rickard WDA, Vickers L, van Riessen A. Performance of fibre reinforced, low density metakaolin geopolymers under simulated fire conditions. Appl. Clay Sci. 2013; 73: 71-77.

5. Van Deventer JSJ, Provis JL, Duxson P. Technical and commercial progress in the adoption of geopolymer cement. Miner. Eng. 2012; 29 (0): 89-104.

6. McLellan BC, Williams RP, Lay J, van Riessen A, Corder GD. Costs and carbon emissions for geopolymer pastes in comparison to ordinary portland cement. J. Clean. Prod 2011; 19 (9–10): 1080-1090.

7. Duxson P, Provis JL. Designing precursors for geopolymer cements. J. Am. Ceram. Soc. 2008; 91 (12): 3864-3869.

8. Brandt AM. Fibre reinforced cement-based (FRC) composites after over 40 years of development in building and civil engineering. Compos. Struct. 2008; 86: 3-9.

9. Davidge RW. Fibre-reinforced ceramics. Composites 1987; 18: 92-98.

10. Lin T, Jia D, Wang M, He P, Liang D. Effects of fibre content on mechanical properties and fracture behaviour of short carbon fibre reinforced geopolymer matrix composites. Bull. Mater. Sci 2009; 32 (1): 7-81.

11. Natali A, Manzi S, Bignozzi MC. Novel fiber-reinforced composite materials based on sustainable geopolymer matrix. Procedia Engineering 2011; 21: 1124-1131.

12. Shaikh FUA. Review of mechanical properties of short fibre reinforced geopolymer composite. Constr. Build. Mater. 2013; 43: 37-49.

13. Aydin S, Baradan B. The effect of fiber properties on high performance alkali-activated slag/silica fume mortars. Composite Part B: Engineering 2013; 45: 63-69.

14. Alomary T, Shaikh FUA, Low IM. Characterisation of cotton fibre-reinforced geopolymer composites. Composite Part B: Engineering 2013; 50: 1-6.

15. Alomary T, Shaikh FUA, Low IM. Synthesis and mechanical properties of cotton fabric reinforced geopolymer composites. Composite Part B: Engineering 2014; 60:36-42.

16. Rickard WDA, van Riessen A. Performance of solid and cellular structured fly ash geopolymers exposed to a simulated fire. Cem. Concr. Comp. 2013.

17. Bernal SA, Bejarano J, Garzón C, Mejía de Gutiérrez R, Delvasto S, Rodríguez E.D. Performance of refractory aluminosilicate particle/fiber-reinforced geopolymer composites. Composites Part B: Engineering 2012; 43 (4): 1919-1928.

18. Vickers L, Rickard WDA, van Riessen A. Strategies to control the high temperature shrinkage of fly ash based geopolymers, Thermochim. acta 2014; 580: 20-27.

19. De Lhoneux B, Akers S, Alderweireldt L, Amiya S, Carmeliet J, Hikasa J. Durability study of PVA fibres in fibre-cement products. Simulation 2002;90: 84.

20. Gyeong-Man K. Fabrication of Bio-Nanocomposite Nanofibers Mimicking the Mineralized Hard Tissues via Electrospinning Process, 2010.

21. Neville AM. Lightweight concrete. in: L.G. limited (Ed.) Properties of Concrete, Harlow, 1995.

22. Wu HC, Sun P. New building materials from fly ash-based lightweight inorganic polymer. Constr. Build. Mater. 2007; 21: 211-217.

23. Arellano Aguilar R, Burciaga Díaz O, Escalante García J. Lightweight concretes of activated metakaolin-fly ash binders, with blast furnace slag aggregates. Constr. Build. Mater. 2010; 24 (7): 1166-1175.

24. Kriven WMB. Preparation of ceramic foams from metakaolin-based geopolymers gels. Ceramic and science proceedings 2008; 29 (10): 98.

25. Medri V, Papa E, Dedecek J, Jirglova H, Benito P, Vaccari A, Landi E. Effect of metallic Si addition on polymerization degree of in situ foamed alkali-aluminosilicates, Ceram. Int. 2013; 39 (7): 7657-7668.

26. Prud'homme E, Michaud P, Joussein E, Peyratout C, Smith A, Arrii-Clacens S, Clacens JM, Rossignol S. Silica fume as porogent agent in geo-materials at low temperature. J. Eur. Ceram. Soc. 2010; 30 (7): 1641-1648.

27. Masi G, Rickard WDA, Vickers L, Bignozzi MC, van Riessen A. A comparison between different foaming methods for the synthesis of light weight geopolymers. Ceramics International 2014; 40:13891-13902.

28. Comrie DC, Kriven WM. Composite cold ceramic geopolymer in a refractory application. Advances in Ceramic Matrix Composites IX 2003; 153: 211-225.

29. Lyon RE, Balaguru P, Foden A, Sorathia U, Davidovits J, Davidovics M. Fire-resistant aluminosilicate composites. Fire Mater. 1997; 21 (2): 67-73.

30. Vaou V, Panias D. Thermal insulating foamy geopolymers from perlite. Miner. Eng. 2010; 23 (14): 1146-1151.

31. Diamond S. A critical comparison of mercury porosimetry and capillary condensation pore size distributions of portland cement pastes. Cem. Concr. Res. 1971; 531-545

32. Feldman RF. Pore structure damage in blended cements caused by mercury intrusion, J. Am. Ceram. Soc. 1984; 67: 30-33.

33. Diamond S. Mercury porosimetry: an inappropriate method for the measurement of pore size distributions in cement-based materials. Cem. Concr. Res. 2000; 30: 1517-1525.

34. Cook RA, Hover KC. Mercury porosimetry of hardened cement paste. Cem. Concr. Res. 1999; 29: 933-943.

35. Gallé C. Effect of drying on cement-based materials pore structure as identified by mercury intrusion porosimetry: a comparative study between oven-, vacuum-, and freeze-drying. Cem. Concr. Res. 2001; 31: 1467-1477.

36. Yu Z, Ye G. The pore structure of cement paste blended with fly ash. Constr. Build. Mat. 2013; 45: 30-35.

37. Ma Y, Hu J, Ye G. The pore structure and permeability of alkali activated fly ash, Fuel 104 (2013)771-780.

38. Lloyd RR. The durability of Inorganic Polymer Cements. Ph.D. Thesis, University of Melbourne, Melbourne, 2008.

39. Kamseu E, Nait-Ali B, Bignozzi MC, Leonelli C, Rossignol S, Smith DS. Bulk composition and microstructure dependence of effective thermal conductivity of porous inorganic polymer cements. J. Eur. Ceram. Soc. 2012; 32: 1593-1603.

40. Bignozzi MC, Manzi S, Lancellotti I, Kemseu E, Barbieri L, Leonelli C. Mix-design and characterization of alkali activated materials based on metakaolin and ladle slag. Appl. Clay Sci. 2013; 73: 78-85.

41. ASTM C39. Standard test method for Compressive Strenght of cylindrical concrete specimens., 2011.

42. ASTM C78. Standard test method for flexural strength of concrete (using simple beam with third-point loading), 2013.

43. ASTM C1421-10. Standard test methods for determination of fracture toughness of advanced ceramics at ambient temperature, 2011.

44. Glatzmaier GC, Ramirez FW. Use of volume averaging for the modeling of thermal properties of porous materials. Chem. Eng. Sci. 1988; 43: 3157-3169.

45. ISO 834. Fire Resistance Tests - Elements of Building Construction - Part 1: General Requirements, 2012.

46. Dias DP, Thaumaturgo C. Fracture toughness of geopolymeric concretes reinforced with basalt fibers. Cem. Concr. Compos. 2005;27 (1): 49-54.

47. Li Z, Zhang Y, Zhou X. Short fiber reinforced geopolymer composites manufactured by extrusion. J. Mater. Civ. Eng. 2005;17 (6): 624-631.

48. Fazio P. Basalt fibra: from earth an ancient material for innovative and modern application. Energia, Ambiente e Innovazione 2011;3: 89-96.

49. Ashby MF, Shercliff H, Cebon D. Materials: engineering, science, processing and design. Butterworth-Heinemann, 2009.

50. Prud'homme E, Michaud P, Joussein E, Peyratout C, Smith A, Rossignol S. Consolidated geo-materials from sand or industrial waste. in: Ceramic Engineering and Science Proceedings 2009; 30: 313.

51. AS 1530.4. Methods for Fire Tests on Building Materials, Components and Structures-Fire-Resistance Test of Elements of Constuctions. Australian Standard 2005.

52. Kim JK, Kim JS, Ha GJ, Kim YY. Tensile and fiber dispersione performance of ECC (enginnered cementitious composites) produced with ground granulated blast furnance slag. Cem. Concr. Res. 2007; 37: 1096-1105.

53. Kanda T, Li VC. Interface property and apparent strength of high-strength hydrophilic fiber in cement matrix. J. Mater. Civ. Eng. 1998; 10: 5-13.

54. Ramachandran BE, Velpari V, Balasubranmanian N. Chemical durability studies on basalt fibres. J. Mater. Sci. 1981; 16: 3393-3397.

G. Masi, W.D.A. Rickard, M.C. Bignozzi, A. van Riessen, The effect of organic and inorganic fibres on the mechanical and thermal properties of aluminate activated geopolymers. Composites Part B: Engineering 76 (2015) 218 – 228
doi:10.1016/j.compositesb.2015.02.023

CAPTIONS:

Fig. 1. Load versus sample extension during the three point bending tests of PVA FRGP.

Fig. 2. Graphs displaying the mechanical properties versus fibre concentration: (A) flexural strength, (B) fracture toughness, (C) work to 1.5 mm of sample extension.

Fig. 3. SEM micrographs showing PVA FRGP and PVA fibres.

Fig. 4. SEM micrographs showing the microstructure of basalt FRGP.

Fig. 5. Graphs displaying flexural strengths after high thermal exposure: (A) PVA and (B) basalt FRGP. Load versus sample extension of (C) PVA and (D) basalt FRGP that have been exposed to different temperatures during three point bending tests.

Fig. 6. SEM images of (A) PVA fibre within the geopolymer matrix and and basalt FRGP after high temperature exposure at (B) 600° C, (C) 700° C, (D) 800° C, (E) 900° C and (F) 1000°C.

Fig. 7. Temperature change with time of each of thermocouples during fire test of (A) PVA and (B) basalt FFRGP. (C) Average cold side temperature during the fire testing of basalt and PVA FFRGP that have been foamed.

Fig. 8. Pore size distributions of different portions of (A) PVA and (B) basalt FFRGP.

Fig. 9. Optical images of the surfaces of the panels after the 180 min fire test: (A) cold side of PVA FFRGP; (B) hot side of PVA FFRGP; (C) cold side of basalt FFRGP; (D) hot side of basalt FFRGP.

G. Masi, W.D.A. Rickard, M.C. Bignozzi, A. van Riessen, The effect of organic and inorganic fibres on the mechanical and thermal properties of aluminate activated geopolymers. Composites Part B: Engineering 76 (2015) 218 – 228
doi:10.1016/j.compositesb.2015.02.023

Fig. 10. Optical images of the cross sections of panels after the fire test: (A) PVA and (B) basalt FFRGP.

G. Masi, W.D.A. Rickard, M.C. Bignozzi, A. van Riessen, The effect of organic and inorganic fibres on the mechanical and thermal properties of aluminate activated geopolymers. Composites Part B: Engineering 76 (2015) 218 – 228
doi:10.1016/j.compositesb.2015.02.023

Table 1. Physical properties of FRGP. Values in parentheses represent the standard deviation of the least significant number to the left.

Fibre type	Fibre content (vol%)	Cured density (g/cm^3)	Diameter of slurry Flow test (mm)	Change in flow from control (%)
-	-	1.72 (2)	81 (2)	0.0
PVA	0.5	1.60 (1)	69 (2)	- 15.4
PVA	1.0	1.61 (1)	47 (2)	- 41.9
Basalt	0.5	1.69 (3)	78 (2)	- 3.7
Basalt	1.0	1.7 (1)	69 (1)	- 26.5

G. Masi, W.D.A. Rickard, M.C. Bignozzi, A. van Riessen, The effect of organic and inorganic fibres on the mechanical and thermal properties of aluminate activated geopolymers. Composites Part B: Engineering 76 (2015) 218 – 228
doi:10.1016/j.compositesb.2015.02.023

Table 2. Density and thermal conductivity of the FFRGP. Values in parentheses represent the standard deviation of the least significant number to the left.

Fibres	Fibre content (vol%)	Foaming method	Foaming agents concentration (wt%)	Thermal conductivity (W/mK)	Density (g/cm^3)
PVA	1.0	Surfactant + H_2O_2	1.0 0.1	0.30 (2)	0.96 (1)
Basalt	1.0	Surfactant + H_2O_2	1.0 0.1	0.38 (2)	1.07 (1)

G. Masi, W.D.A. Rickard, M.C. Bignozzi, A. van Riessen, The effect of organic and inorganic fibres on the mechanical and thermal properties of aluminate activated geopolymers. Composites Part B: Engineering 76 (2015) 218 – 228
doi:10.1016/j.compositesb.2015.02.023

Table 3. Physical properties of the fire tested panels; times and temperatures at critical points during the fire testing of FFRGP samples.

Fibre type	vol%	Mass loss (%)	Time for T (average)>165 ^{o}C (min)	Time for T (any)>205 ^{o}C (min)
PVA	1.0	18	99	111
Basalt	1.0	15	80	88

G. Masi, W.D.A. Rickard, M.C. Bignozzi, A. van Riessen, The effect of organic and inorganic fibres on the mechanical and thermal properties of aluminate activated geopolymers. Composites Part B: Engineering 76 (2015) 218 – 228
doi:10.1016/j.compositesb.2015.02.023

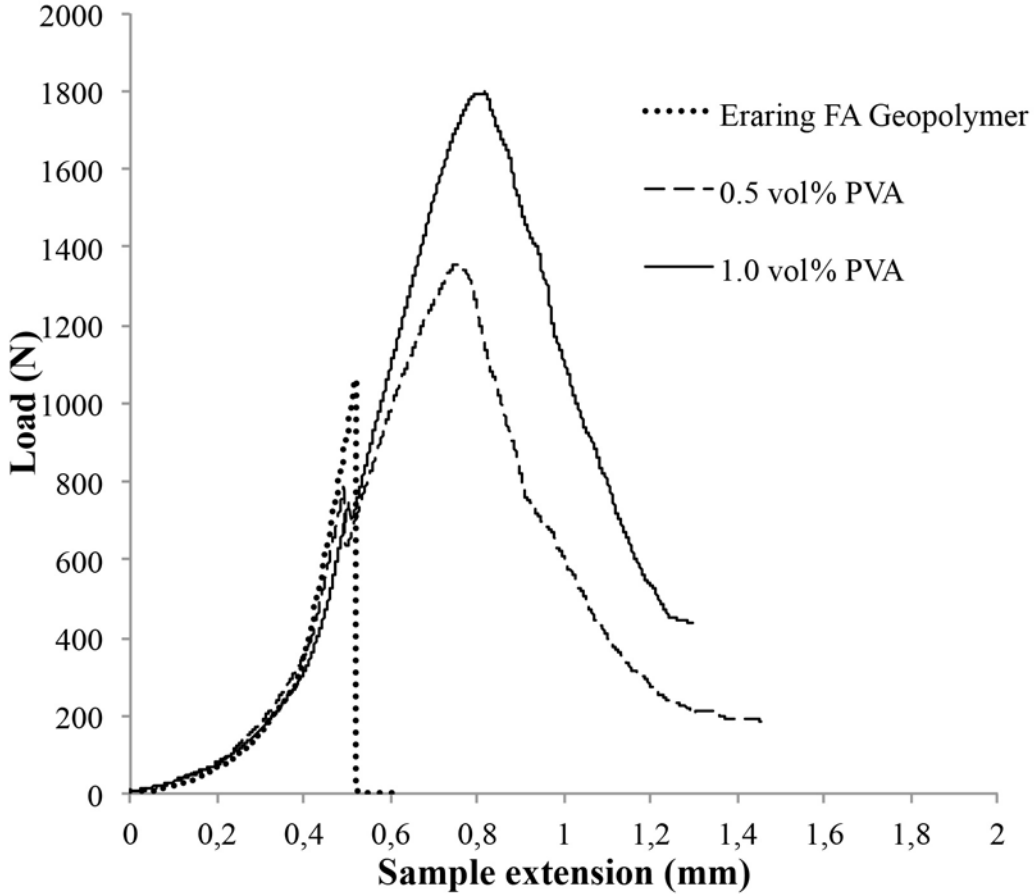

Fig. 1

G. Masi, W.D.A. Rickard, M.C. Bignozzi, A. van Riessen, The effect of organic and inorganic fibres on the mechanical and thermal properties of aluminate activated geopolymers. Composites Part B: Engineering 76 (2015) 218 – 228
doi:10.1016/j.compositesb.2015.02.023

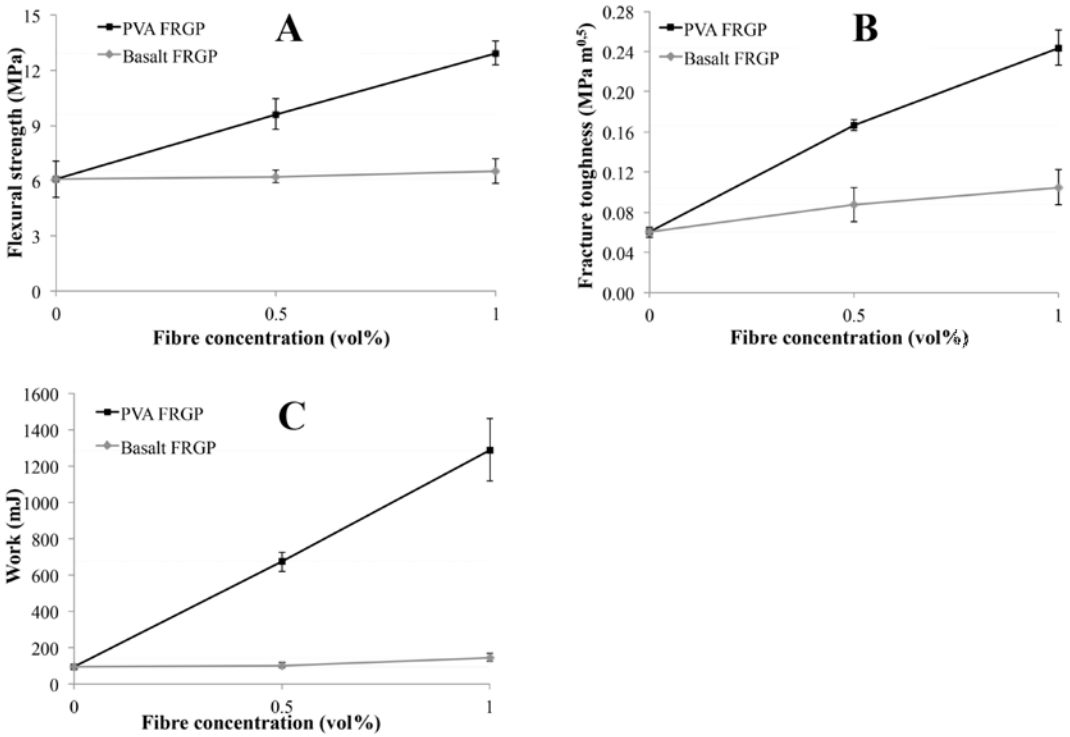

Fig. 2

G. Masi, W.D.A. Rickard, M.C. Bignozzi, A. van Riessen, The effect of organic and inorganic fibres on the mechanical and thermal properties of aluminate activated geopolymers. Composites Part B: Engineering 76 (2015) 218 – 228
doi:10.1016/j.compositesb.2015.02.023

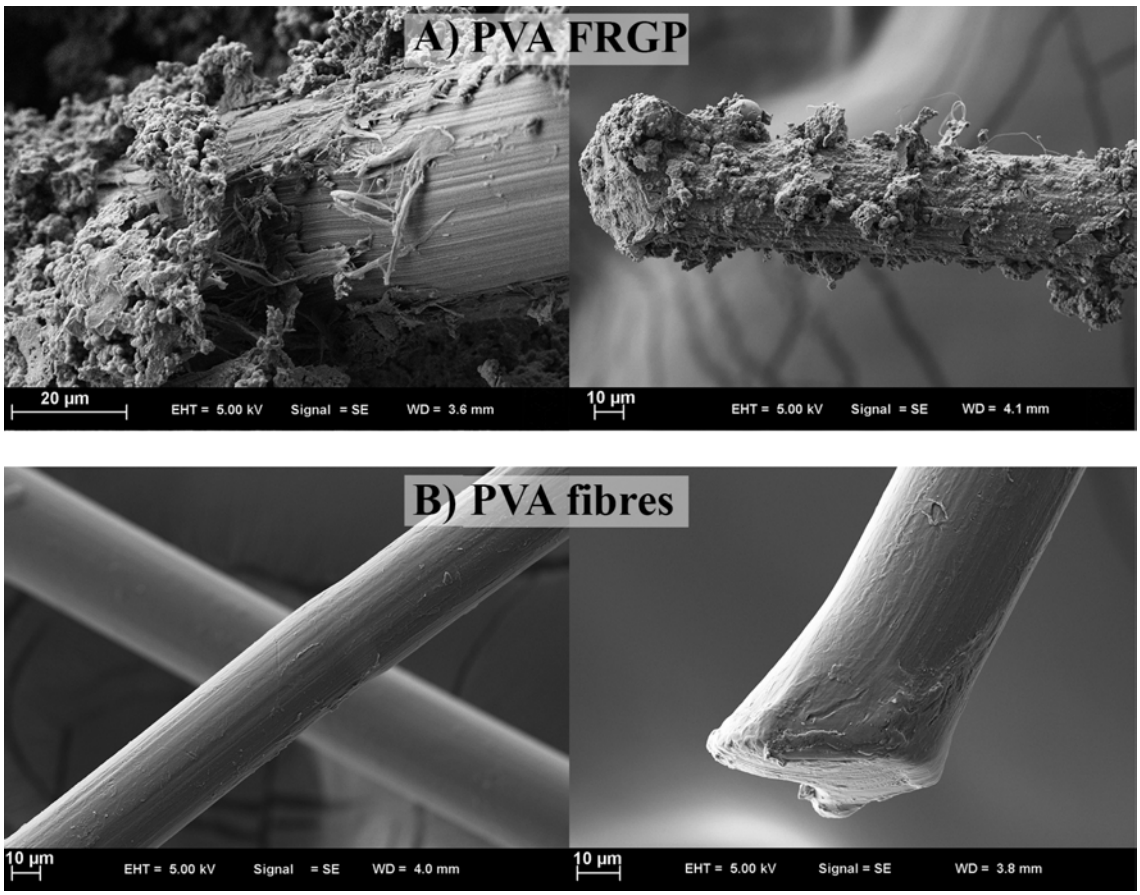

Fig. 3

G. Masi, W.D.A. Rickard, M.C. Bignozzi, A. van Riessen, The effect of organic and inorganic fibres on the mechanical and thermal properties of aluminate activated geopolymers. Composites Part B: Engineering 76 (2015) 218 – 228
doi:10.1016/j.compositesb.2015.02.023

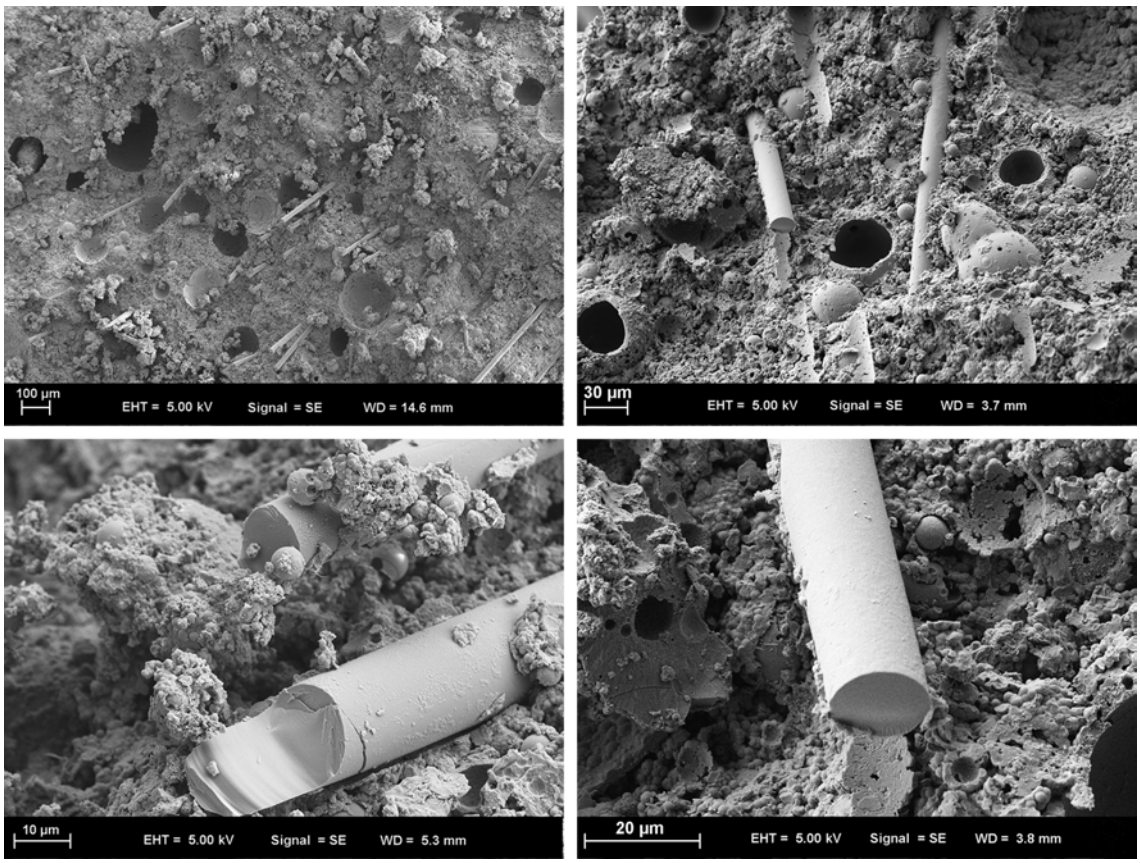

Fig. 4

G. Masi, W.D.A. Rickard, M.C. Bignozzi, A. van Riessen, The effect of organic and inorganic fibres on the mechanical and thermal properties of aluminate activated geopolymers. Composites Part B: Engineering 76 (2015) 218 – 228
doi:10.1016/j.compositesb.2015.02.023

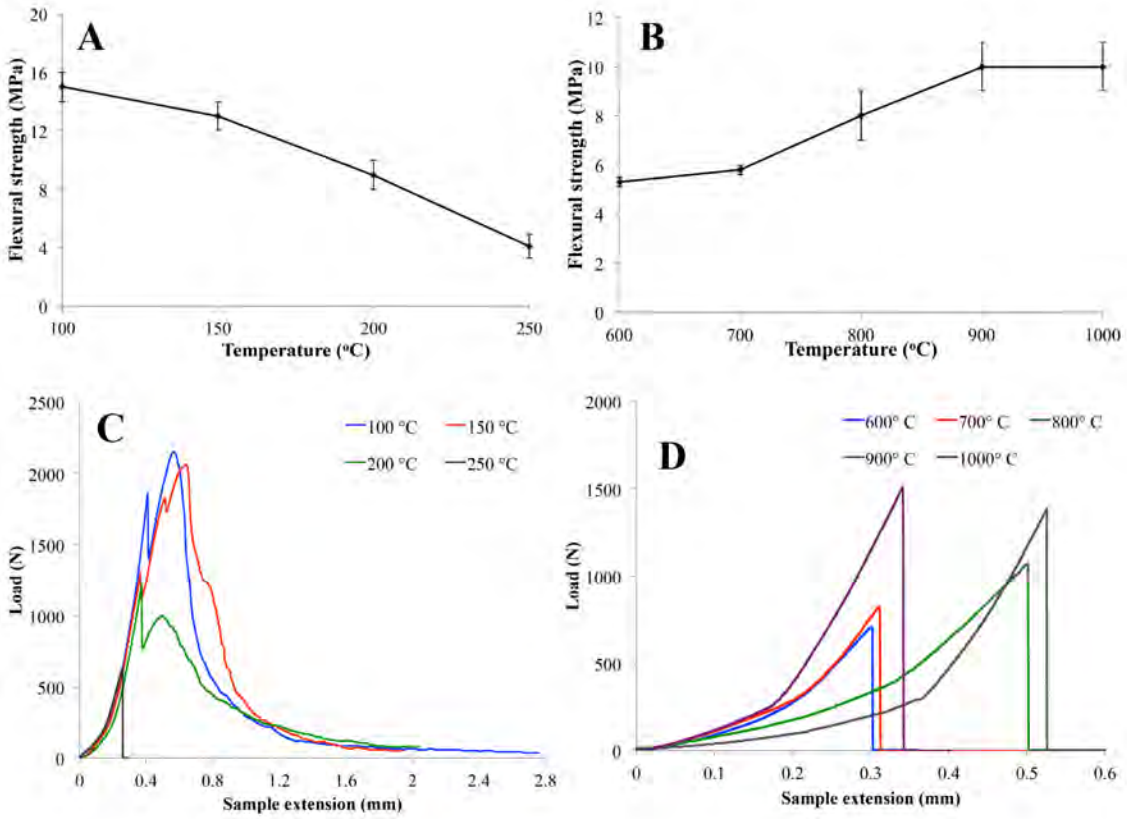

Fig. 5

G. Masi, W.D.A. Rickard, M.C. Bignozzi, A. van Riessen, The effect of organic and inorganic fibres on the mechanical and thermal properties of aluminate activated geopolymers. Composites Part B: Engineering 76 (2015) 218 – 228
doi:10.1016/j.compositesb.2015.02.023

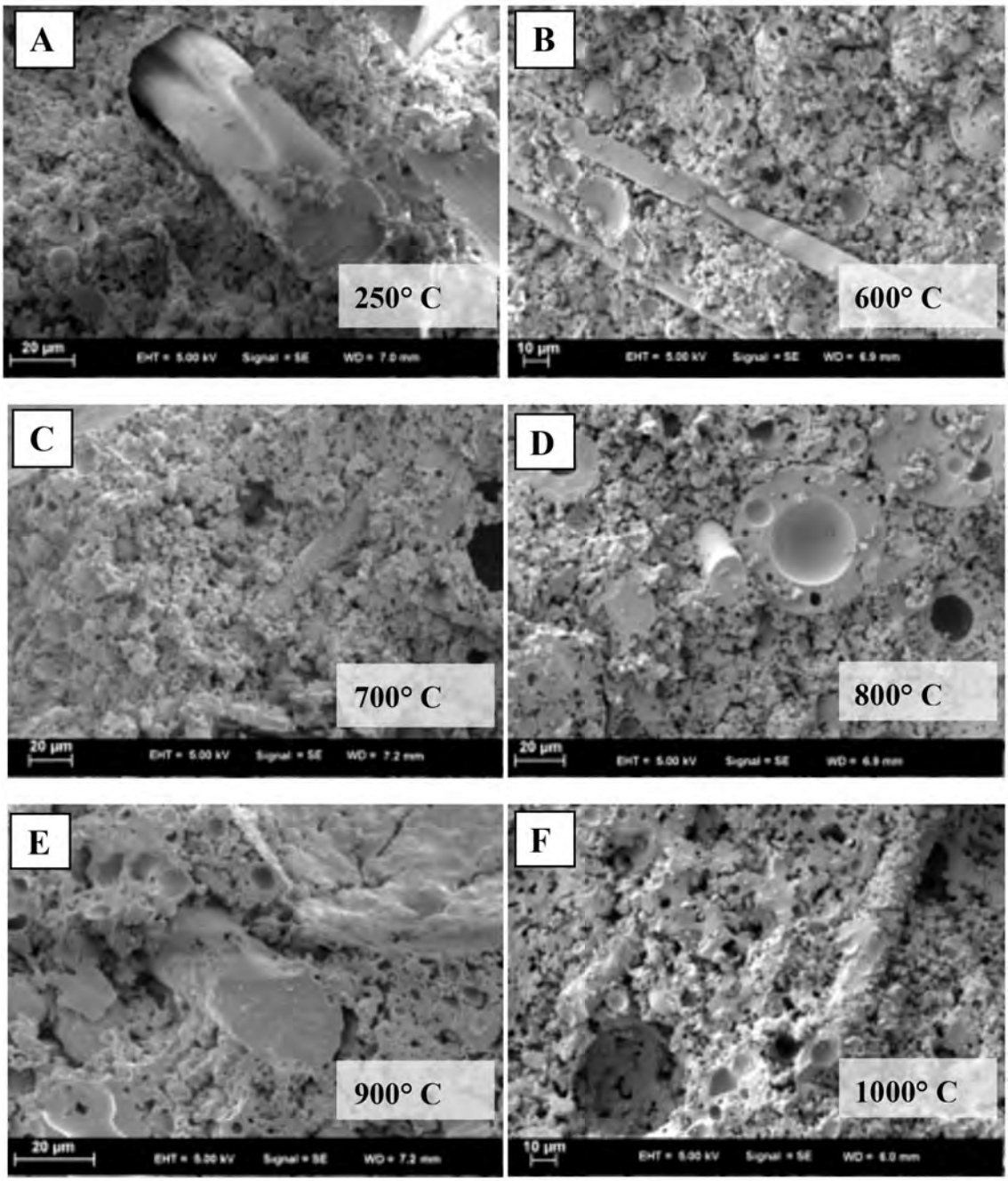

Fig. 6

G. Masi, W.D.A. Rickard, M.C. Bignozzi, A. van Riessen, The effect of organic and inorganic fibres on the mechanical and thermal properties of aluminate activated geopolymers. Composites Part B: Engineering 76 (2015) 218 – 228
doi:10.1016/j.compositesb.2015.02.023

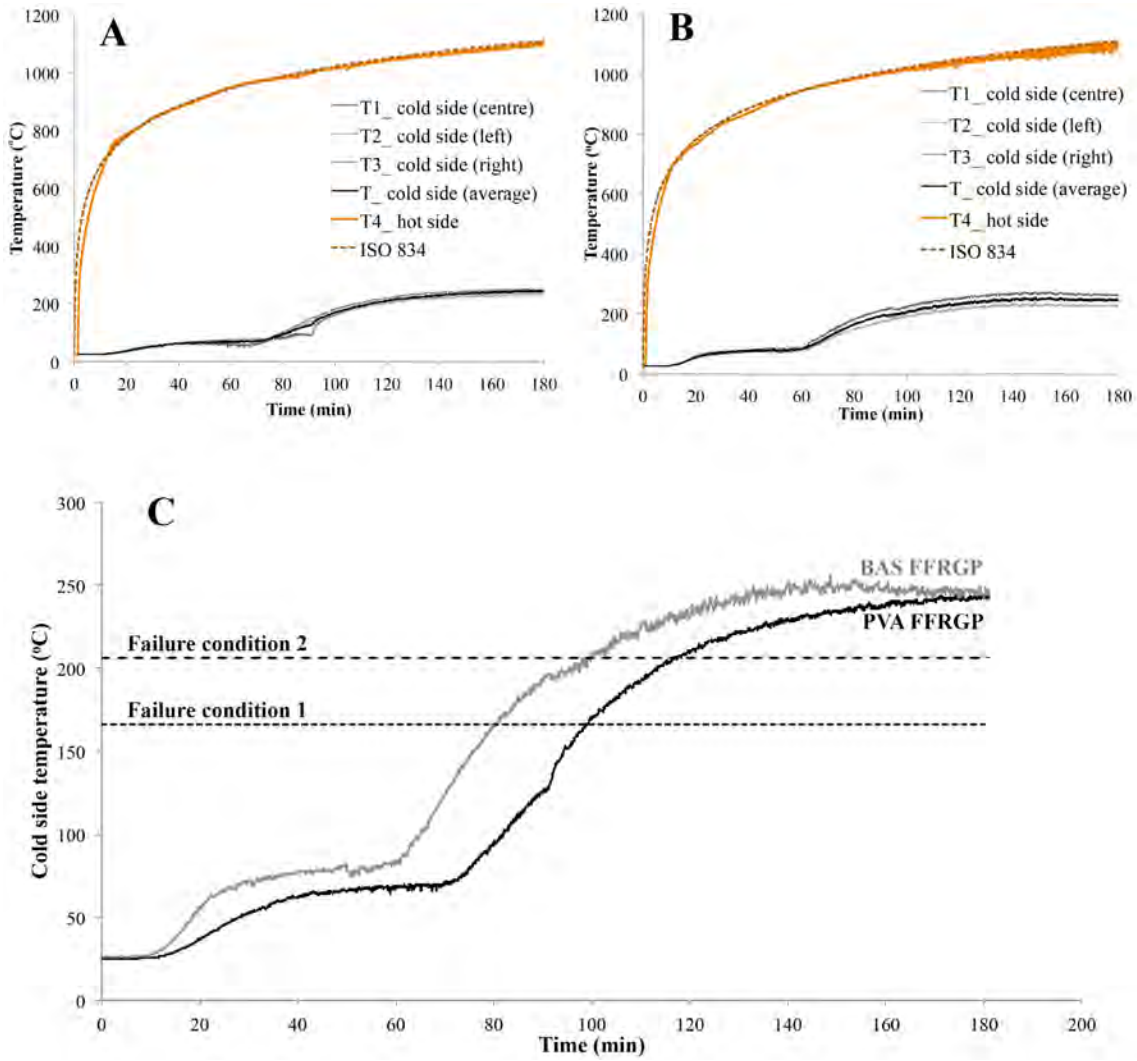

Fig. 7

G. Masi, W.D.A. Rickard, M.C. Bignozzi, A. van Riessen, The effect of organic and inorganic fibres on the mechanical and thermal properties of aluminate activated geopolymers. Composites Part B: Engineering 76 (2015) 218 – 228
doi:10.1016/j.compositesb.2015.02.023

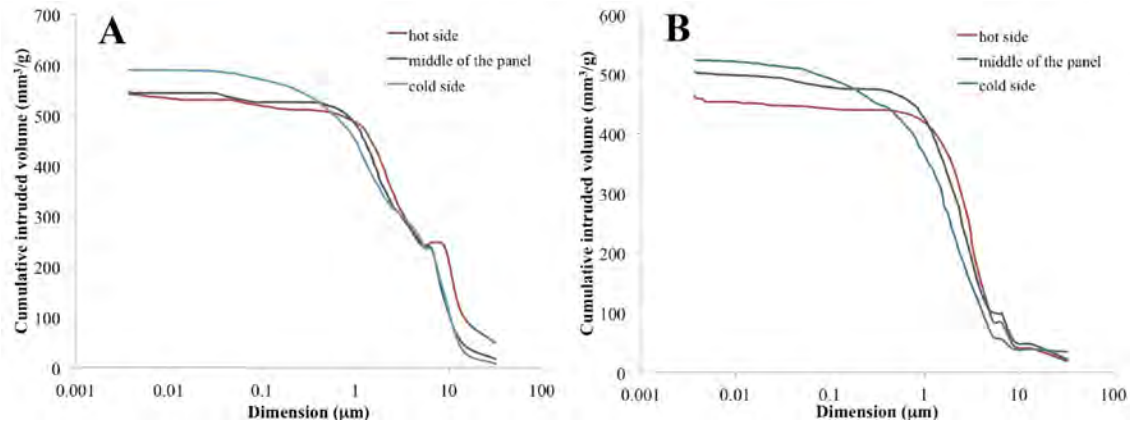

Fig. 8

G. Masi, W.D.A. Rickard, M.C. Bignozzi, A. van Riessen, The effect of organic and inorganic fibres on the mechanical and thermal properties of aluminate activated geopolymers. Composites Part B: Engineering 76 (2015) 218 – 228
doi:10.1016/j.compositesb.2015.02.023

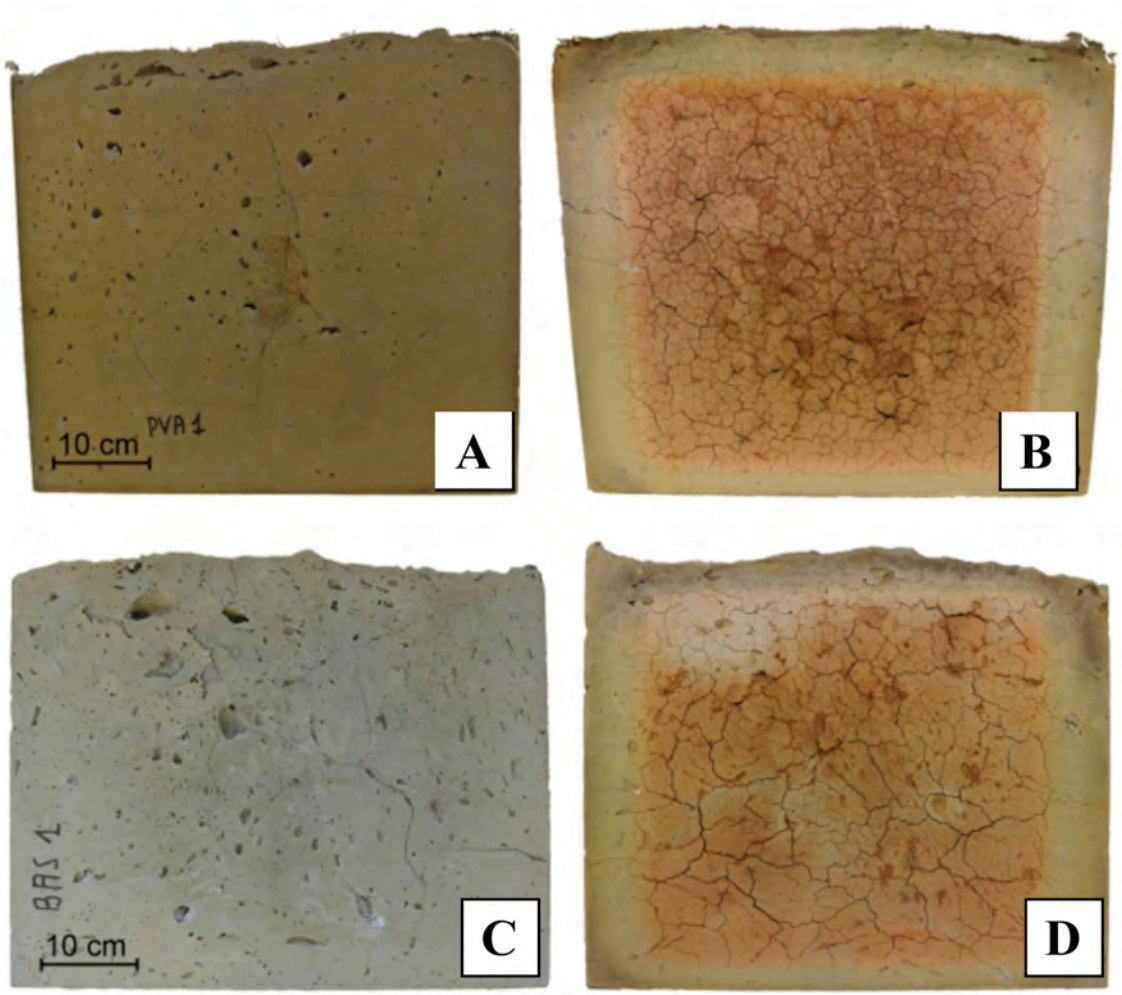

Fig. 9

G. Masi, W.D.A. Rickard, M.C. Bignozzi, A. van Riessen, The effect of organic and inorganic fibres on the mechanical and thermal properties of aluminate activated geopolymers. Composites Part B: Engineering 76 (2015) 218 – 228
doi:10.1016/j.compositesb.2015.02.023

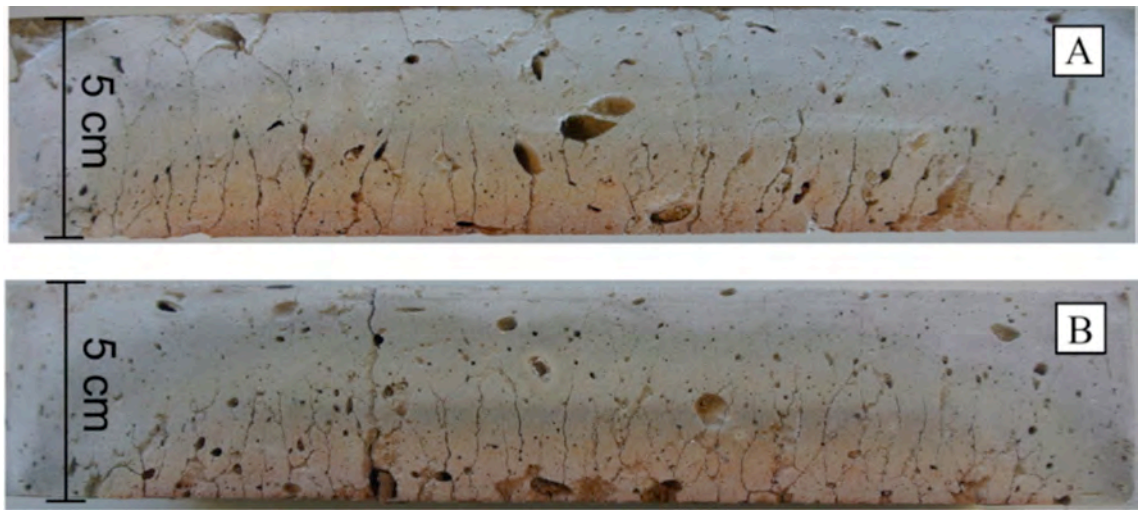

Fig. 10